

962

815

TECHNICAL MEMORANDUMS

NATIONAL ADVISORY COMMITTEE FOR AERONAUTICS



3 1176 00113 4908

-----  
No. 1000  
-----

THE TEMPERATURE OF UNHEATED BODIES IN

A HIGH-SPEED GAS STREAM

By E. Eckert and W. Weise

Forschung auf dem Gebiete des Ingenieurwesens  
Vol. 12, no. 1, January-February 1941

1113  
11141

-----  
Washington  
December 1941

NATIONAL ADVISORY COMMITTEE FOR AERONAUTICS

TECHNICAL MEMORANDUM NO. 1000

THE TEMPERATURE OF UNHEATED BODIES IN  
A HIGH-SPEED GAS STREAM\*

By E. Eckert and W. Weise

SUMMARY

The present report deals with temperature measurements on cylinders of 0.2 to 3 millimeters diameter in longitudinal and transverse air flow at speeds of 100 to 300 meters per second. Within the explored test range, that is, the probable laminar-boundary-layer region, the temperature of cylinders in axial flow is practically independent of the speed and in good agreement with Pohlhausen's theoretical values; whereas, in transverse flow, cylinders of certain diameter manifest a close relationship with speed, the ratio of the temperature above the air of the body to the adiabatic stagnation temperature first decreases with rising speed and then rises again from a Mach number of 0.6. The importance of this "specific temperature" of the body for heat-transfer studies at high speed is discussed.

INTRODUCTION

A body that neither receives nor gives off heat, assumes the temperature of the air in a flow at low speed. But at airspeeds of the order of sonic velocity its temperature is higher, as in that instance the temperature rise, because of the air's being slowed down to zero at the surface of the body and so causing its temperature to rise partly through damming, partly through internal friction, has already reached appreciable values. This phenomenon is of technical importance in many respects. When the temperature in a flowing gas is recorded, the temperature of the thermometer, of course, registers the same increase; hence the latter must be known if the true

---

\*"Die Temperatur unbeheizter Körper in einem Gasstrom hoher Geschwindigkeit." Forschung auf dem Gebiete des Ingenieurwesens, vol. 12, no. 1, Jan.-Feb. 1941, pp. 40-50.

gas temperature is to be obtained from the thermometer reading. The knowledge of the temperature of the unheated body in air flow is a requisite for heat-transfer estimates. If the body, because of heating or cooling, has a higher or lower temperature than it would have unheated, it gives off or absorbs heat. On aircraft these phenomena become significant by wing-skin cooling, insulation of pressure cabins, and icing.

The temperature which the unheated body assumes in the air stream is hereinafter termed its "specific temperature." Aside from several older experiments with thermocouples stretched along the axis of Laval nozzles, the available data on specific temperature measurements are limited to those by Meissner (reference 1). And these deal only with a thermocouple of a certain form that had been used for heat transfer measurements. For this reason we made several fundamental tests for determining the specific temperature on simple body shapes, the study of which was permitted by the small air stream available. After the experiments were completed a report by Hilton (reference 2) on similar tests appeared in print.

#### HEAT-TRANSFER CONSTANTS AT HIGH SPEEDS. (REFERENCE 3)

The equations for the stationary process of heat exchange and motion in a gas read:

$$\text{Continuity equation } \operatorname{div}(\rho \underline{w}) = 0 \quad (1)$$

Equation of motion. (reference 3a)

$$\rho (\underline{w} \operatorname{grad}) \underline{w} = 2 \operatorname{grad}(\eta \operatorname{def} \underline{w}) - \frac{2}{3} \operatorname{grad}(\eta \operatorname{div} \underline{w}) - \operatorname{grad} p \quad (2)$$

Energy equation (reference 3a)

$$\rho g (\underline{w} \operatorname{grad} c_p) - \underline{w} \operatorname{grad} p = \operatorname{div}(\lambda \operatorname{grad} \theta) + \eta \text{dissipation function} \left[ \left( \frac{\partial w_x}{\partial x} \right)^2 + \dots \right] \quad (3)$$

where  $\underline{w}$  is the speed vector,  $p$  the pressure,  $\theta$  the temperature,  $\rho$  the density,  $\eta$  the viscosity,  $\lambda$  the heat conductivity,  $c_p$  the specific heat of the gas, and  $g$  the acceleration due to gravity.

At low speeds the term with the dissipation function

can be discounted. And if the values  $\rho$ ,  $\eta$ ,  $c_p$ , and  $\lambda$  themselves are treated as constant, similarity of speed, temperature, and pressure is afforded for two processes when the boundaries of the problem are geometrically similar, when the temperature and velocity fields are similar at the boundaries and the two constants  $Re = w_0 l / \nu$  and  $Pr = \nu / a$  ( $\nu = \eta / \rho$  kinematic viscosity,  $a = \lambda / \rho g c_p$ , temperature conductivity) each have the same magnitude; where  $w_0$  is a typical speed to be read from the boundary conditions and  $l$  a representative length. Since the equations contain only temperature and pressure gradients, it is sufficient for the two temperature and pressure fields at the boundaries if the differences relative to a chosen reference point are similar for the two processes. Then the excess temperatures and excess pressures in the temperature and pressure fields which would be obtained as solution of equations (1) to (3) are themselves similar over the same reference point.

At high speeds the term with the dissipation function may not be disregarded. Even though the material values including density  $\rho$  are still treated as constant, the above conditions from the comparison of the term in the energy equation containing the dissipation function, we supplemented by a further constant, which, after multiplication by the Reynolds number, takes the form  $c_p g \theta_0 / w_0^2$ , where  $\theta_0$  is again a representative high temperature taken from the boundary conditions. The temperature rise caused by adiabatic damming of the gas flow at speed  $w_0$  on the speed zero, is  $\theta_{ad} =$

$$\frac{w_0^2}{2 g c_p}$$

So the above constant can equally be employed in

the form  $\theta_0 / \theta_{ad}$ . In the temperature field the excess temperatures  $\theta$  above the chosen reference point at similarly located points can then be nondimensionally written in the form

$$\frac{\theta}{\theta_0} = f \left( Re, Pr, \frac{\theta_0}{\theta_{ad}} \right) \quad (4)$$

whence follows the dimensionless heat transfer coefficient  $Nu$  by formation of the temperature gradient at the wall

$$Nu = \frac{\alpha l}{\lambda} = \left( \frac{\partial \frac{\theta}{\theta_0}}{\partial \frac{n}{l}} \right)_w = f_1 \left( Re, Pr, \frac{\theta_0}{\theta_{ad}} \right) \quad (5)$$

( $\alpha$  heat transfer coefficient,  $n$  direction at right angles to the wall). In the case where there is no exchange of heat with the wall, equating the differential

quotient  $\left( \frac{\delta \frac{\theta_e}{l}}{\delta \frac{n}{l}} \right)$  to zero affords

$$\frac{\theta_e}{\theta_{ad}} = f_2(\text{Re}, \text{Pr})$$

which defines the excess temperature  $\theta_e$  of the unheated wall. Pohlhausen (reference 4) has computed the temperature  $\theta_e$  reached by a plate-shape thermometer in a rapid gas flow, when the assumption justified here is made (reference 5) that the density  $\rho$  is constant and the boundary layer laminar. The result can be made to agree with the foregoing by

$$\frac{\theta_e}{\theta_{ad}} = f(\text{Pr}) \quad (6)$$

The relationship with the Reynolds number ceases for laminar flow, as indicated in table 1. For  $\text{Pr} = 0.6$  to 2,

$\frac{\theta_e}{\theta_{ad}} = \sqrt{\text{Pr}}$  is a close approximation.

TABLE 1.— TEMPERATURE OF PLATE IN AXIAL FLOW WITH LAMINAR BOUNDARY LAYER (POHLHAUSEN)

Pr	0.6	0.7	0.8	0.9	1	1.1	10	100	1000
$\theta_e/\theta_{ad}$	0.77	0.835	0.895	0.95	1	1.05	2.96	6.7	12.9

In the case of variable density, as it almost always does in reality at high speeds, the previous equation must be supplemented by the equation of state  $\rho = f(p, T)$ , which restricts the number of similar cases considerably. The study hereinafter is confined to gases that follow the equation of state  $p = g\rho RT$ , with  $R$  the gas constant and  $T$  the absolute gas temperature. At constant  $\rho$  similarity of excess temperature and pressure above a

chosen reference point was sufficient for the compared processes. Now by variable  $\rho$  the density fields themselves shall be similar. But this supplementary demand can be reconciled with the equation of state only in the presence of similitude of absolute temperature and pressure, not merely for the excess temperatures and pressures.

An illustrative example of this fact in the heat transfer of gas on the pipe wall is given. The gas in the entrance section of the pipe has the constant temperature  $T_{g_0}$ , the pipe wall throughout its length the constant temperature  $T_w$ . Then the fields of excess temperature  $\theta_0 = T_{g_0} - T_w$  at the boundary are always similar for all possible cases, irrespective of the magnitude of  $T_{g_0}$  and  $T_w$  individually, and the field of the dimensionless excess temperatures can be represented by an equation of the form of equation (4), so long as  $\rho$  is constant. On the other hand, the fields of the absolute temperature maintain similitude only if  $T_w/T_{g_0}$  or  $\theta_0/T_{g_0}$  is constant. Only so long as this condition at the boundary is satisfied does equation (4) hold for the temperature field.

So for arbitrary temperatures it must be complemented by the parameter quantity  $\theta_0/T_{g_0}$  and read

$$\theta/\theta_0 = f(\text{Re}, \text{Pr}, \theta_0/\theta_{ad}, \theta_0/T_{g_0})$$

Then constant  $\theta_0/\theta_{ad}$  itself can be transformed by multiplication with the reciprocal value of the temperature ratio  $\theta_0/T_{g_0}$ :

$$\frac{\theta_0}{\theta_{ad}} \frac{T_{g_0}}{\theta_0} = \frac{2 g c_p \theta_0 T_{g_0}}{w_0^2 \theta_0} = \frac{2 g c_p T_{g_0}}{w_0^2} \quad (7)$$

The sonic velocity of the gas in question at the entrance section is given by

$$a = \sqrt{g \kappa R T_{g_0}} = \sqrt{g(\kappa - 1)c_p T_{g_0}}$$

whence

$$\frac{\theta_o}{\theta_{ad}} \frac{T_{g_o}}{\theta_o} = \left( \frac{a}{w_o} \right)^2 \frac{2}{\kappa - 1}$$

The term  $w_o/a$  is the Mach number  $Ma$  and  $(\kappa - 1)$  is constant for gas at a certain Prandtl number. Hence the above equation can equally be written as

$$\frac{\theta_o}{\theta_o} = f_1 \left( Re, Pr, Ma, \frac{\theta_o}{T_{g_o}} \right)^*$$

The specific temperature of a body in the flow follows in the same manner, by putting the temperature gradient at its surface equal to zero. The result then is

$$\frac{\theta_e}{T_{g_o}} = f_2(Re, Pr, Ma)$$

or, when dividing the equation on both sides by the Mach number to squares and effecting slight changes at the left side:

$$\frac{\theta_e}{\theta_{ad}} = f_3(Re, Pr, Ma)$$

For the determination of the heat-transfer coefficient at high speed additional considerations are dictated. Of itself the heat-transfer coefficient  $\alpha$  enters the calculations through an arbitrary equation

$$\alpha \theta_o = \lambda \left( \frac{\partial \theta}{\partial n} \right)_w$$

This proves appropriate to the extent that for forced convection and low speed the so-defined heat-transfer coefficient is independent of the temperature difference  $\theta_o$ , as long as the material quantities can be treated as constant, for the temperature does not occur in Nusselt's constant  $Nu = \alpha l/\lambda$  formed with the heat transfer coefficient or in the others ( $Re, Pr$ ). By free

---

\*With  $\theta_o/T_{g_o}$  the temperature relationship of the other values  $(\eta, \lambda, c_p)$  itself is afforded, as far as it can be represented by power functions of the absolute temperature.

convection, to be sure, a relation with temperature difference  $\theta_0$  still exists because of Grashof's constant ( $Gr = l^3 g \beta \theta_0 / \nu^2$ ,  $\beta =$  coefficient of expansion), but this is known to be small (in free flow past a plate or a pipe  $\frac{1}{\sqrt{\theta_0}}$ ). Although a heat-transfer coefficient is defined at high speeds, the aim here also must be to achieve independence, or at least, little dependence from the excess temperature. Such is certainly not the case if, at low speeds,  $\alpha$  is referred to the temperature difference of the wall relative to the flowing gas ( $T_{g_0} - T_w$ ) with the equation

$$q = \alpha(T_{g_0} - T_w) = \lambda \left( \frac{\partial \theta}{\partial n} \right)_w \quad (8)$$

where  $q$  is heat transfer per unit area per unit time. Figure 1a to 1c shows the temperature curve ( $T_g$ ) in the boundary layer at high speeds. Outside the boundary layer the gas is to have a temperature  $T_{g_0}$ . If the wall neither receives nor gives off heat ( $q = 0$ ), it assumes, according to the foregoing, the specific temperature  $T_e$ . Then the temperature in the boundary layer must have the curve shown in figure 1b. But if the wall temperature is higher than the specific temperature (fig. 1a), the wall transmits heat to the gas; if it is lower the wall absorbs heat (fig. c). The tangent of angle  $\epsilon$  is, according to equation (8), proportional to this heat volume  $q$ . For the unheated wall ( $q = 0$ ), which assumes a temperature  $T_w = T_e > T_{g_0}$  (fig. 1b),  $\alpha = 0$  is obtained, according to equation (8). On the other hand, there must then be a wall temperature  $T_w = T_{g_0}$  at which the gas gives off heat, that is,  $q \neq 0$ . This case is illustrated in figure 1c. In this instance  $\alpha = \infty$ . There is therefore a marked dependence on the temperature difference. The only way to avoid this is to define  $\alpha$  as follows:

$$q = \alpha(T_e - T_w) = \lambda \left( \frac{\partial \theta}{\partial n} \right)_w \quad (9)$$

Then the heat-transfer coefficient is independent of the temperature at least in first approximation. The premise for computing the heat transfer then is, of course, knowledge of the specific temperature.



## THE SPECIFIC TEMPERATURE

Schirokow (reference 6) in extending Prandtl's boundary layer theory of heat transfer to high speeds arrived at the following heat-transfer formula in turbulent pipe flow:

$$\text{Nu} = K \frac{\xi}{8} \frac{\text{Re Pr}}{1 + \frac{w_g}{w_o} (\text{Pr} - 1)} \quad (10)$$

$\left( \xi = \frac{2 \Delta p}{\rho w_o^2 l} \right)$  resistance of pipe,  $w_o$  mean flow velocity

in pipe,  $w_g$  speed at boundary between laminar boundary layer and turbulent nuclear flow). This equation differs from Prandtl's formula by the quantity  $K$ , which has the following significance:

$$K = 1 + \frac{w_o^2}{2 g c_p \theta_o} \left[ 1 + \left( \frac{w_g}{w_o} \right)^2 (\text{Pr} - 1) \right] \quad (11)$$

The heat transfer coefficient in the Nusselt constant of equation (10) is referred to temperature  $\theta_o = T_{g_o} - T_w$ .

Thus the heat transfer  $q$ , per unit area per unit time is

$$q = \frac{\lambda}{\alpha} \left\{ \theta_o + \frac{w_o^2}{2 g c_p} \left[ 1 + \left( \frac{w_g}{w_o} \right)^2 (\text{Pr} - 1) \right] \right\} \frac{\xi}{8} \frac{\text{Re Pr}}{1 + \frac{w_g}{w_o} (\text{Pr} - 1)} \quad (12)$$

This heat  $q$  is zero when the term within the braces equals zero. Here the excess temperature of the unheated pipe over that of the flowing gas follows at

$$\theta_o = T_e - T_{g_o} = \frac{w_o^2}{2 g c_p} \left[ 1 + \left( \frac{w_g}{w_o} \right)^2 (\text{Pr} - 1) \right] \quad (13)$$

In turn, temperature  $T_e$  can be re-entered in equation (12):

$$q = \frac{\lambda}{\alpha} (T_e - T_w) \frac{\xi}{8} \frac{\text{Re Pr}}{1 + \frac{w_g}{w_o} (\text{Pr} - 1)} \quad (14)$$

When, therefore, the heat-transfer coefficient, according to equation (9), is referred to  $T_e - T_w$ , the temperature difference at both sides of the equation cancels, thus leaving the same formula as at low speeds:

$$\text{Nu} = \frac{\xi}{8} \frac{\text{Re Pr}}{1 + \frac{w_g}{w_0} (\text{Pr} - 1)} \quad (15)$$

Thus the heat-transfer coefficient defined according to equation (9) is, according to this theory, actually independent of the temperature. The same result is obtained with an exact mathematical treatment of the heat transfer on a flat plate (reference 5).

Equation (13) was evaluated in figure 2, with Ten Bosch's version of speed ratio  $w_g/w_0$  (reference 7.) This same equation as equation (14), wherein the resistance coefficient  $\xi$  must be replaced by the referred shearing stress at the wall, applies equally to the specific temperature of a plate in axial turbulent flow. Figure 3 shows the temperature variation of a plate with well-sharpened leading edge plotted against the Reynolds number formed with the distance from the plate circumference. Such a plate develops first a laminar boundary layer which at a critical Reynolds number becomes turbulent. In interference-free inflow this critical Reynolds number is  $5 \times 10^5$ . To this number Pohlhausen's theory is then applicable (reference 4). From there on, equation (13) was resorted to, the speed ratio  $w_g/w_0$  being again computed in the same manner as by Ten Bosch.\*

#### SET-UP AND MEASUREMENTS

The tests included circular cylinders and various pitotlike shapes at different temperature and speeds approaching that of sound (fig. 4).

---

\*Ten Bosch gives the speed ratio for a turbulent boundary layer starting at plate leading edge;  $w_g/w_0$  was computed in the same manner for a turbulent boundary layer originating from laminar flow at  $\text{Re} = 5 \times 10^5$ .

The circular cylinders in transverse flow (fig. 4, A) consisted of brass tubes of 1, 1.5, 2, and 3 millimeters diameter and 0.1 millimeter wall thickness. The tubes a were filled in the center with solder b, over a length of about 6 millimeters, holding the thermocouple wires c of manganese-constantan of 0.2 millimeter size, electrically insulated by thin glass tubing d. The brass tubes were just long enough to extend a little to either side beyond the air stream and served as leads for the glass tubes held in stirrup f (fig. 5). The thin brass tubes in conjunction with the inserted glass tubes were intended to keep the heat losses at a minimum by deflection from the test station. This was achieved with the smaller diameters; whereas no measurements with greater differences between specific temperature and room temperature could be made on the tubes with 2 and 3 millimeters diameter because of the appearance of instrumental errors due to heat dissipation at low air speed. The thermocouples themselves, carefully butt-soldered to prevent thickening at the seam, served as cylinders of 0.2 and 0.5 millimeter diameter.

The pitot-shaped bodies (fig. 4, B to E), also of brass tubing a of 0.1 millimeter wall thickness and 2 and 6 millimeters diameter, carried the junction b in front (C and E) or a little distant from the tip (B and D); two were rounded off (D and E), the other two had a tip (B and C).

The air was supplied by a single-stage rotary blower (Klein-Schanzlin and Becker Company) of 400 cubic meters per hour capacity. An oil separator, cooler, and electric heating element were installed in the pressure line. In the cooler the air was cooled to approximately room temperature and dried by the removal of the water; by regulating the heat output it could be heated again to 50° C. The pressure line b is joined by the pressure chamber a (fig. 5), from which the air escaped to the outside through a rectangular nozzle c of 26x11 square millimeters cross section. The test bodies d were held on a stirrup e in the air stream above the nozzle. For the measurements on thermocouples in axial flow, the latter were inserted through the nozzle and fastened to a stirrup f in the pressure chamber. The excess pressure in the pressure chamber was measured with a mercury manometer the air temperature with a thermocouple g mounted crosswise before the nozzle. For measuring the specific temperature, the thermocouple soldered into the tube was connected opposite to that disposed in the pressure cham-

ber, thus affording the difference  $\Delta t$  between the air temperature in the chamber and the specific temperature direct. The measurement was accomplished by compensation with a Lindeck-Rothe instrument (reference 8). Evaluation of the measurements further requires the knowledge of the temperature in the air stream. Since this is not directly obtainable, it was computed from the pressure chamber temperature recorded with thermocouple  $t_g$  on the assumption that the air in the nozzle expands adiabatically up to outside pressure. This certainly holds true for the core of the air stream because the boundary layer in which the friction losses and contingent effects due to heat dissipation on the nozzle wall occur has surely not advanced as far as the stream center in the short distance over the nozzle where the test body was mounted (about 5 to 10 mm). This assumption can be checked readily by measuring the dynamic pressure with a pitot tube substituted at the place where the tubes are otherwise. If the change from pressure-into-motion energy is accomplished without loss, the pitot tube must register the chamber pressure which is not reached if losses occur. This measurement disclosed at 558 millimeters mercury column, excess chamber pressure, a difference of 2 millimeters mercury column, or 0.3 percent between it and the pressure registered on the pitot tube. The same conditions prevailed at the other speeds in the flow.

The computed air temperature in the jet therefore indicates the true value very accurately, and the measured temperature in the chamber is equal to the temperature which the air in the jet assumes by adiabatic damping. The airspeed in the jet can be computed in the same manner from the measured excess pressure in the pressure chamber on the basis of adiabatic expansion.

#### RESULTS OF TESTS

The results with the cylinder in transverse flow have been compiled in table 2. It contains, besides the measured and computed values, the airspeed  $w$  and the adiabatic temperature rise,  $\theta_{ad}$ , the temperature ratio  $\theta_e/\theta_{ad}$ , that is, the excess temperature of the body over the air in ratio to the adiabatic temperature rise, and lastly the Reynolds number and the Mach number. The calculation of the constants was based on the kinematic viscosity and the sonic velocity at mean boundary layer temperature about the cylinder, that is, at temperature  $t_i - (\Delta t + \theta_{ad})/2$ .

Each wire diameter was subjected to three tests: In the first the air temperature in the chamber was kept at around 50° C, in the second to about room temperature, in the third the air temperature in the pressure chamber was so regulated for each speed that the specific temperature of the cylinder equaled room temperature, hence precluding instrumental errors due to dissipation. On the tubes with more than 1 millimeter diameter these errors at 50° air temperature in the chamber were already so pronounced that these measurements were omitted in the tabulation. And since their ratio to jet width (11 mm) is also unfavorably great at the larger diameters, the test data are more uncertain than on the smaller tubes.

In figure 6 the temperature ratio  $\rho_e/\rho_{ad}$  is plotted against the air speed, in figure 7 against Mach's number. The line drawn through the points of each test series is identified by the number of the test series in table 2. The relationship between temperature ratio and speed is very plain, especially for the 0.5 and 1 millimeter diameters. The measurements at different pressure chamber temperatures in relation to Mach's number are fairly well grouped about a single curve. The still-existing differences between the separate lines range within experimental accuracy. A closer study of the curves shows that as a rule the test series with high air temperature place lowest, those with the air in the chamber at room temperature, highest, and those with the adapted chamber temperature in between. This shows that the differences are chiefly due to heat dissipation, which were unavoidable by the small jet dimensions.

Plotted against the Reynolds number the differences between the  $\rho_e/\rho_{ad}$  values of the individual test series is even greater than when plotted against the speed.

As a check on whether the flat aspect of the  $\rho_e/\rho_{ad}$  lines for diameters from 1.5 millimeters upward was due to the small air-jet dimensions, the same tests were duplicated on two larger nozzles (14 x 39 millimeters and 19 x 44 millimeters). For 0.2, 0.5, and 1 millimeter cylinder diameter the so obtained test data checked closely with those in figure 7; whereas for the 2 and 3 millimeter cylinder diameter the temperature ratios  $\rho_e/\rho_{ad}$  measured in the greater air streams place lower than in figure 7 and approach the aspect of the  $\rho_e/\rho_{ad}$  lines for 0.5 and 1 millimeter, and so confirms the suspicion that

its flat aspect is due to the limited jet dimensions.

The principal constant defining the process is, according to figure 7, the Mach number, supplemented by the Reynolds number effect, otherwise the  $\rho_e/\rho_{ad}$  values for 0.2 millimeter wire diameter and those for 0.5 and 1 millimeter would coincide. The upward bend at first of the decreasing  $\rho_e/\rho_{ad}$  values with ascending Mach number, made especially plain by the 0.5 and 1 millimeter diameter although the other cylinder diameters also indicate it, is probably attributable to the fact that at the corresponding Mach number the highest speed occurring on the cylinder circumference equals the speed of sound. In the potential flow of an incompressible medium the maximum speed at the cylinder circumference is twice as high as the flow velocity. In the compressible medium it is even higher. Kaplan (reference 9) arrived at 0.425 as Mach's number formed with the flow velocity, where the maximum speed equals the speed of sound. The Mach number for which  $\rho_e/\rho_{ad}$  is minimum in the graphs, is located at about 0.6. This is due to the fact that, because of the boundary layer separation, the maximum speed at the cylinder is lower than in the potential flow.

Figure 8 represents the test data for axial wires of 0.2, 0.5, and 2 millimeters diameter, with the chamber temperature about equal to room temperature. Forming Reynolds number with the wire length from the beginning of the narrowest nozzle section to the junction, it ranges between  $0.5 \times 10^5$  and  $5 \times 10^5$  in the measurements. In interference-free flow the boundary layer is laminar within this zone. For air at room temperature, which has a Prandtl number  $Pr = 0.714$  (reference 10), figure 3 and table 1 give a temperature ratio  $\rho_e/\rho_{ad}$  of 0.842, which is in very good agreement with the measurements. At the quoted Reynolds numbers the thickness of the laminar boundary layer at the cylinder amounts to about 1/10 millimeter. In spite of the value, no longer small in respect to its diameter with the weakest wire, the curvature of the boundary layer has no effect on the specific temperature.

The tests with the pitotlike bodies B to E (fig. 4) had the same aspect as on the axial cylinder. The temperature  $\rho_e/\rho_{ad}$  was practically independent of the speed. For forms D and E the ratio  $\rho_e/\rho_{ad}$  amounted to

about 0.8, on forms B and D it had about the same magnitude as on the axially placed cylinder of figure 8 (0.83 at low speeds with a slight rise to 0.86 at 300 m/s). Such bodies are therefore quite suitable for temperature recording in high-speed air flow (reference 11).

#### COMPARISON WITH OTHER TEST DATA

Hilton's measurements (reference 2) in the high-speed wind tunnel were made on a plate thermometer of poorly heat-conducting material (Tufnol). His  $\frac{t_e}{t_{ad}}$  values of 0.87 to 0.89 at Reynolds numbers of around  $0.8 \times 10^5$  to  $3.6 \times 10^5$  are a little higher than our own on axial wires. He also tested streamline and circular cylinders of the same material in transverse flow, and measured the local specific temperature. He also noticed discontinuities in relation to the speed and likewise attributed these to the appearance of local supersonic speeds in combination with shock waves. Measuring on a circular cylinder of 6 millimeters diameter the specific temperature at different points, he found a  $\frac{t_e}{t_{ad}}$  ratio of about 0.88 at the forward stagnation point, of 0.46 at the side, and 0.22 at the rear. This result likewise is indicative of the fact that the flatness of the curves in figure 7 for cylinder diameters in excess of 1 millimeter is attributable to the small jet dimensions.

Translation by J. Vanier,  
National Advisory Committee  
for Aeronautics.

## REFERENCES

1. Meissner, W.: Temperaturmessung in rasch strömenden gasen. Forsch. Ing.-Wes., vol. 9, 1938, pp. 213-18.
2. Hilton, W. F.: Thermal Effects on Bodies in an Air Stream. Proc. Royal Soc., vol. 168, 1938, pp. 43-56.
3. Gröber, H., and Erk, S.: Die Grundgesetze der Wärmeübertragung, Berlin, 1933, pp. 121 and 188.  
Busemann, A.: Gasdynamik, in W. Wien und F. Harms, Handbuch Exp. Phys., vol. 4, pt. 1, Leipzig, 1931.  
Schmidt, Ernst: Einführung in die technische Thermodynamik, Berlin, 1936, p. 268.
- 3a. Busemann, A.: Gasdynamik, in W. Wien und F. Harms, Handbuch Exp. Phys., vol. 4, pt. 1, Leipzig, 1931, pp. 350-56. (See reference 3, where def  $w$  is a tensor of the deformation speed.)
4. Pohlhausen, E.: Z.f.a.M.M., vol. 1, 1921, pp. 115-21.
5. Eckert, E., and Drewitz, O.: Forsch. Ing.-Wes., vol. 11, 1940, no. 3, pp. 116-24.
6. Schirokow, M.: Tech. Physics USSR, vol. 3, 1936, pp. 1020-27.
7. Ten Bosch, M.: Die Wärmeübertragung, Berlin, 1936, p. 112.
8. Knoblauch, O., and Henky, K.: Anleitung zu genauen technischen Temperaturmessungen. München, 1926.
9. Kaplan, C.: Two-Dimensional Subsonic Compressible Flow Past Elliptic Cylinders. Rep. No. 624, NACA, 1938.
10. Henning, F.: Wärmetechn. Richtwerte, Berlin, 1938.
11. Eckert, E.: Temperature Recording in High-Speed Gases. T.M. No. 983, NACA, 1941.



Table 2.- Specific temperature of cylinders in transverse flow.

Test No.	Cylinder dia. mm	Chamber temperature $t_c$ °C.	Room temperature $t_R$ °C	Chamber press. $\Delta p_i$ mm QS	Atmosph. press. $p_a$ mm QS	Temp.-Diff. chamber/spec. temp. $\Delta t$ °C	Air speed $w$ m/s	Adiab. Temperature drop $\theta_{ad}$ °C	$\frac{\theta_e}{\theta_{ad}} = 1 - \frac{\Delta t}{\theta_{ad}}$	Re	Ma
1		49,9		91	755,0	2,45	176 <sup>10A</sup>	10,3	0,762	2020	0,494
		49,9		253	755,0	7,56	221 <sup>10A</sup>	25,8	0,695	2680	0,630
		49,9		409	755,0	9,55	275	37,4 <sup>V</sup>	0,745	3500	0,793
		49,9		552	755,0	11,8	306 <sup>V</sup>	46,5 <sup>V</sup>	0,746	4030	0,890
		49,9		706	755,0	13,1	335 <sup>V</sup>	55,4 <sup>V</sup>	0,764	4550	0,983
2	0,2	15,9		79	752,0	2,22	127 <sup>12A</sup>	8,25	0,731	1790	0,378
		15,7		139	752,0	3,73	165	13,7	0,725	2370	0,491
		14,8		206	752,0	5,49	197	19,2	0,715	2910	0,591
		15,2		278	752,0	7,30	225	25,0	0,709	3380	0,680
		14,9		327	752,0	8,17	238	28,2	0,711	3670	0,722
		14,8		417	752,0	7,82	262	33,9	0,770	4110	0,799
		15,2		458	752,0	7,99	272	36,6	0,782	4300	0,831
		15,3		528	752,0	9,74	287	40,7	0,761	4620	0,882
		15,3		652	752,0	10,24	314	47,4	0,784	5190	0,971
		3		20,4	18,4	* 84	766,0	2,33	133 <sup>V</sup>	8,81 <sup>V</sup>	0,735
22,1	18,6			140	766,0	3,68	168	13,8	0,735	2410	0,498
23,6	18,6			196	766,0	4,80	193	18,8	0,745	2820	0,585
24,3	18,6			260	766,0	6,05	220	24,0	0,751	3290	0,659
26,5	18,6			334	766,0	7,32	243	29,3	0,751	3710	0,732
27,4	18,7			404	766,0	7,94	263	34,2	0,768	4100	0,797
27,7	18,6			471	766,0	8,50	278	38,3	0,778	4400	0,846
28,6	18,6			523	766,0	10,18	290	41,6	0,756	4670	0,887
29,7	18,6			690	766,0	10,83	320	50,8	0,787	5330	0,987
4				53,4		82	743,0	3,54	140 <sup>V</sup>	9,5 <sup>V</sup>	0,626
		53,4		255	742,0	11,75	233	26,6	0,559	6590	0,667
		53,4		425	741,0	11,51	283	39,2	0,707	8750	0,813
		53,4		592	740,0	11,10	318	50,3	0,781	10150	0,922
		53,4		705	740,0	14,09	339	56,8	0,759	11150	0,991
5	0,5	17,7		80	751,0	2,64	130	8,4	0,692	4500	0,384
		17,7		144	751,0	5,47	169 <sup>V</sup>	14,2 <sup>V</sup>	0,622	6010	0,503
		17,7		202	751,0	7,78	197	19,1	0,595	7240	0,591
		17,7		239	751,0	8,78	211	22,0	0,606	7800	0,634
		18,2		302	751,0	10,1	234	27,1	0,630	8800	0,706
		17,9		370	751,0	10,1	252	31,4	0,682	9640	0,765
		18,8		454	751,0	9,27	274	36,7	0,750	10580	0,833
		17,7		536	751,0	8,69	288	41,3	0,792	11360	0,881
		17,2		649	751,0	9,68	309	47,3	0,797	12510	0,954
6		21,1	17,6	83	766,0	3,24	132	8,6	0,627	4580	0,387
		23,6	18,1	140	766,0	5,89	168	13,9	0,578	5870	0,495
		27,0	18,2	198	766,0	8,32	197	19,2	0,567	6910	0,580
		28,3	18,4	263	766,0	10,4	222	24,4	0,573	7910	0,657
		31,1	18,4	330	766,0	12,0	244	29,8	0,595	8700	0,722
		30,7	18,3	409	766,0	11,7	265	34,9	0,663	9650	0,789
		29,0	18,7	463	766,0	11,8	277	38,0	0,714	10280	0,829
		28,4	18,7	530	766,0	9,62	290	41,9	0,771	10910	0,876
		31,4	18,9	683	766,0	12,4	319	50,7	0,755	12210	0,962
7		49,9		252	756,0	10,1	228	25,5	0,602	14240	0,651
		49,9		405	756,0	10,2	274	37,1	0,725	17740	0,793
		49,9		579	756,0	10,4	312	47,9	0,783	20850	0,940
		49,9		708	756,0	10,8	335	55,7	0,806	22980	0,981
8	1	12,5		80	750,0	2,70	129 <sup>V</sup>	8,2 <sup>V</sup>	0,665	9810	0,384
		12,5		135	750,0	4,99	163	13,1	0,627	11940	0,489
		12,1		201	749,0	7,56	195	18,8	0,602	14710	0,589
		12,2		272	749,0	8,95	222	24,2	0,633	17190	0,676
		12,5		342	749,0	9,18	242	29,1	0,688	18950	0,739
		12,9		408	749,0	9,07	260	33,4	0,731	20580	0,796
		12,2		465	749,0	8,19	271	36,5	0,778	21720	0,833
		12,7		530	749,0	8,19	284	40,5	0,800	22980	0,875
		13,0		596	749,0	8,44	298	44,0	0,819	24450	0,922
		13,2		652	749,0	8,44	308	46,9	0,821	25500	0,955

Test No.	Cylinder diameter mm	Chamber temperature $t_c$ °C	Room temperature $t_R$ °C	Chamber press. $\Delta p_1$ mm QS	Atmosph. press. $p_a$ mm QS	Temp.-Diff. chamber/spec. temp. $\Delta t$ °C	Air speed $w$ m/s	Adiab. Temperature drop $\vartheta_{ad}$ °C	$\frac{\vartheta_e}{\vartheta_{ad}} = 1 - \frac{\Delta t}{\vartheta_{ad}}$	Re	Ma
9	1	19,8	16,9	83	766,5	3,24	132	8,6	0,625	9230	0,388
		22,4	17,2	139	766,5	5,76	168	14,0	0,590	11820	0,495
		26,5	17,6	198	766,5	8,33	197	19,1	0,566	13850	0,581
		27,2	16,8	266	766,5	10,6	223	24,6	0,566	16020	0,661
		29,3	18,2	327	766,5	11,4	243	29,3	0,611	17530	0,721
		31,1	18,6	405	766,5	11,5	264	34,4	0,666	19160	0,785
		29,0	18,8	462	766,5	10,7	277	37,9	0,717	20570	0,829
		30,1	19,0	530	766,5	10,4	292	42,1	0,752	21870	0,875
		30,3	19,6	647	766,5	10,3	313	48,7	0,787	23820	0,943
10	1,5	11,8		81	761,5	2,35	129	8,2	0,715	14100	0,384
		11,8		137	761,5	3,80	163	13,2	0,713	18200	0,489
		13,7		200	761,5	4,82	194	18,6	0,741	21800	0,583
		13,7		254	761,5	5,67	217	22,6	0,750	24800	0,655
		14,4		327	761,5	6,64	237	27,8	0,762	27500	0,719
		14,4		402	761,5	7,16	257	32,7	0,782	30400	0,784
		14,1		467	761,5	7,80	271	36,4	0,786	32600	0,830
		14,9		514	761,5	7,94	282	39,4	0,799	34200	0,864
15,4		637	761,5	8,24	304	45,9	0,820	37500	0,937		
11		18,3	16,4	78	765,0	2,40	128	8,1	0,706	13400	0,377
		20,9	16,0	136	765,0	4,16	166	13,5	0,692	17500	0,490
		22,1	15,9	200	765,0	6,05	195	18,8	0,682	20900	0,578
		25,2	18,7	266	765,0	6,28	222	24,4	0,743	23800	0,658
		25,8	18,7	336	765,0	6,65	244	29,4	0,775	26600	0,726
		27,2	19,0	400	765,0	7,25	262	34,0	0,788	28700	0,781
		27,0	19,4	463	765,0	7,70	276	37,8	0,797	30700	0,826
		27,9	19,6	540	765,0	8,20	292	42,4	0,807	32900	0,877
		28,7	19,8	655	765,0	8,83	314	48,8	0,819	36000	0,948
12		34,4	17,3	62	761,0	2,64	122	7,4	0,643	15400	0,350
		36,2	18,1	120	761,0	4,21	160	12,6	0,668	20300	0,460
		41,5	18,9	210	761,0	6,53	207	21,2	0,693	26400	0,595
		44,0	19,7	287	761,0	7,36	235	27,9	0,736	30200	0,677
		44,4	19,9	404	761,0	8,72	271	36,3	0,760	35700	0,787
		44,5	19,6	501	761,0	9,08	293	42,5	0,787	39400	0,855
		44,4	19,6	608	761,0	9,58	314	48,9	0,804	43300	0,922
13	2	19,4	18,2	79	752,5	2,30	180	8,3	0,724	17900	0,382
		22,2	18,5	144	752,5	3,83	171	14,4	0,735	23600	0,504
		23,7	18,6	205	752,5	5,12	200	19,8	0,742	28300	0,591
		25,4	18,6	266	752,5	6,16	224	24,8	0,752	31700	0,663
		26,1	18,7	335	752,5	7,28	246	29,9	0,757	35300	0,732
		27,6	18,9	402	752,5	8,00	264	34,5	0,768	38100	0,788
		27,8	18,6	463	752,5	8,40	278	38,3	0,781	40700	0,831
		27,4	19,0	535	752,5	8,79	293	42,6	0,794	43700	0,881
28,0	19,0	685	752,5	9,32	320	50,6	0,816	48600	0,969		
14	3	12,2		85	762,0	1,64	131	8,5	0,808	28500	0,390
		12,2		143	762,0	2,87	166	13,6	0,790	36900	0,497
		12,7		200	762,0	3,90	194	18,5	0,790	43800	0,583
		13,3		267	762,0	5,04	219	23,7	0,788	50400	0,660
		13,7		335	762,0	5,90	239	28,3	0,792	55600	0,725
		14,2		400	762,0	6,70	257	32,7	0,793	60900	0,783
		14,9		461	762,0	7,12	271	36,2	0,803	64800	0,827
		15,4		543	762,0	7,62	287	40,9	0,814	69700	0,880
		16,0		631	762,0	8,12	302	45,6	0,822	74200	0,930
15		18,9	17,8	81	764,5	1,78	131	8,4	0,789	27400	0,385
		20,8	18,6	141	764,5	3,18	168	13,9	0,772	36000	0,495
		22,8	17,2	266	764,5	5,68	221	24,2	0,746	48200	0,657
		24,0	17,1	335	764,5	7,15	243	29,4	0,757	53500	0,725
		25,0	16,9	407	764,5	8,00	263	34,2	0,767	58700	0,788
		25,4	16,9	476	764,5	8,75	279	38,5	0,773	63100	0,838
		25,8	16,8	531	764,5	9,07	290	41,7	0,783	66400	0,874
		26,2	17,0	674	764,5	9,70	315	49,2	0,803	73800	0,956
		20,6	17,2	202	765,0	4,37	196	19,0	0,771	42400	0,582

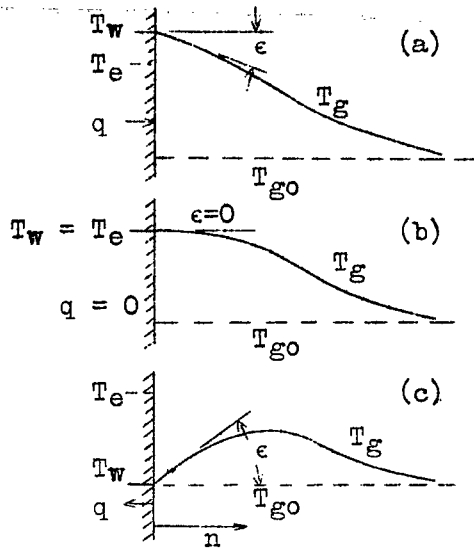


Figure 1.- Temperature variation in the boundary layer of a high-speed gas flow.

Figure 2.- Specific temperature at the wall of a pipe in high-speed gas flow (Schirokow).  $\delta_e$  = excess temperature of body over air stream,  $\delta_{ad}$  = adiabatic temperature rise.

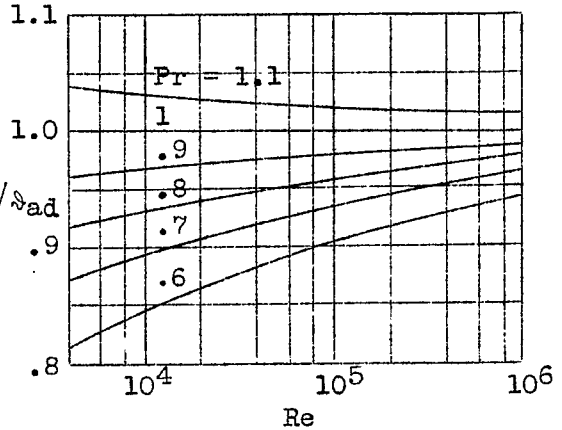
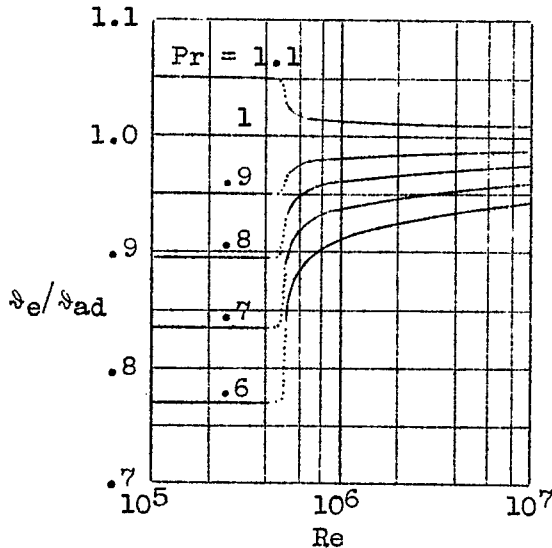


Figure 3.- Specific temperature of flat plate in high-speed axial flow (Schirokow). Transition of laminar to turbulent boundary layer flow at  $Re = 5 \times 10^5$ .



$$2.237 \times \# \text{ m/s} = \# \text{ M.P.H}$$

$$3.937 \times 10^{-2} \times \# \text{ mm} = \# \text{ IN}$$

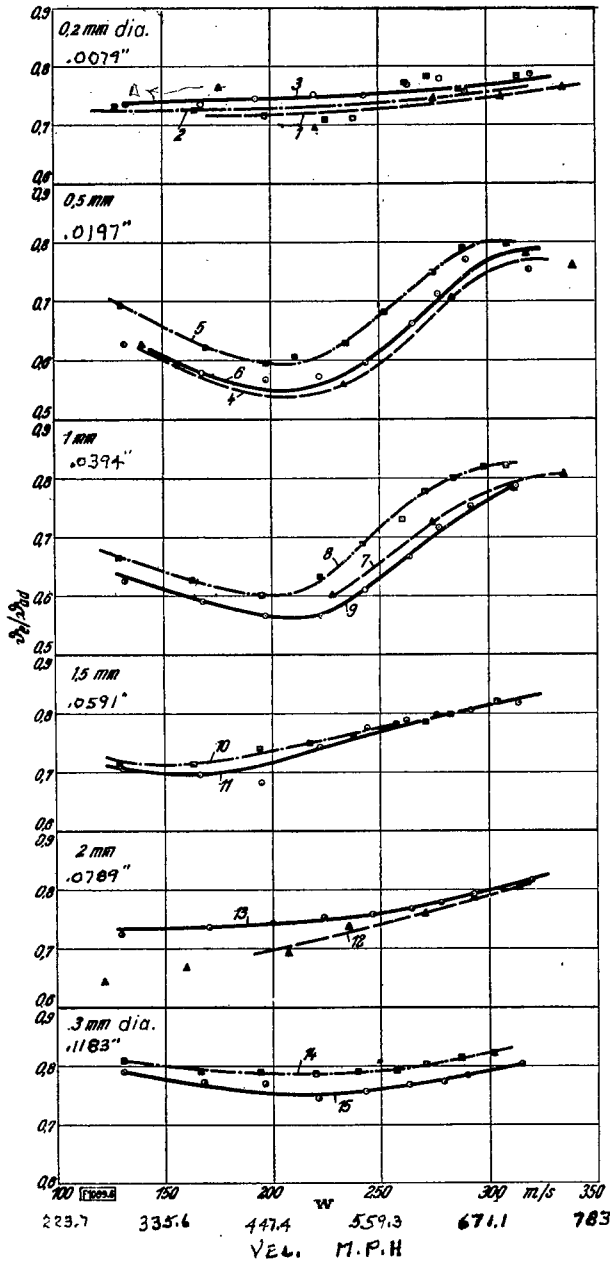


Figure 6.- Ratio  $v_e/v_{ad}$  for cylinder in transverse flow plotted against air speed.

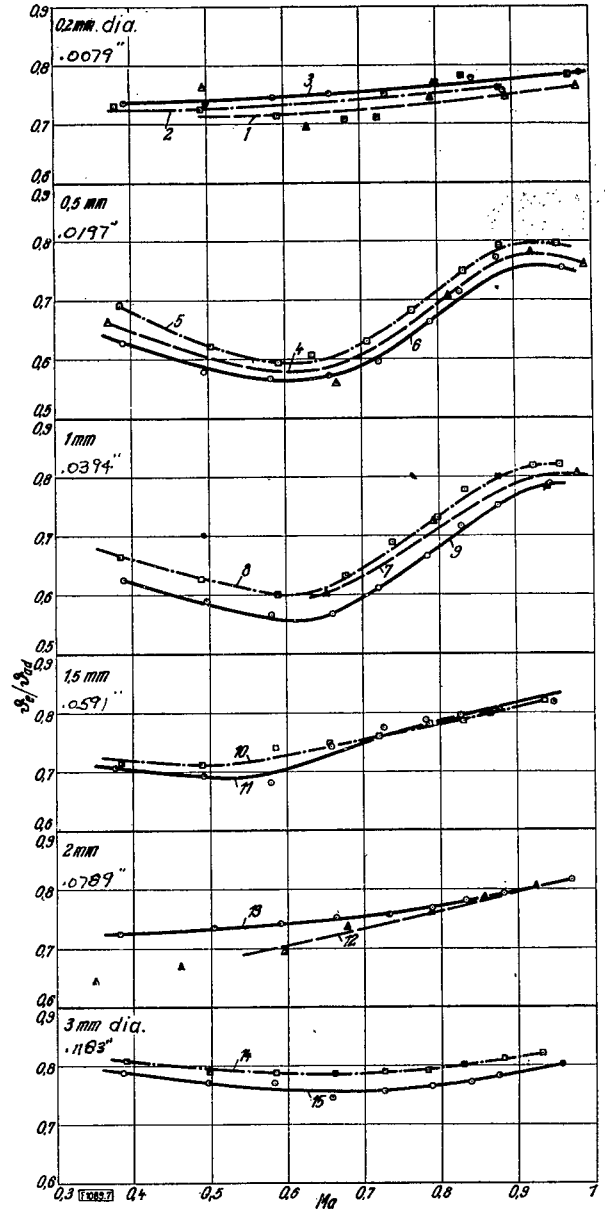


Figure 7.- Ratio  $v_e/v_{ad}$  for cylinder in transverse flow plotted against Mach's number.